



HAL
open science

Influence of pressure (100Pa–100Mpa) on the pyrolysis of an alkane at moderate temperature (603K–723K): Experiments and kinetic modeling

R. Bounaceur, F. Lannuzel, R. Michels, G. Scacchi, P.-m. Marquaire, V. Burklé-Vitzthum

► To cite this version:

R. Bounaceur, F. Lannuzel, R. Michels, G. Scacchi, P.-m. Marquaire, et al.. Influence of pressure (100Pa–100Mpa) on the pyrolysis of an alkane at moderate temperature (603K–723K): Experiments and kinetic modeling. *Journal of Analytical and Applied Pyrolysis*, 2016, 122, pp.442 - 451. 10.1016/j.jaap.2016.10.022 . hal-01412810

HAL Id: hal-01412810

<https://hal.science/hal-01412810v1>

Submitted on 31 Jan 2022

HAL is a multi-disciplinary open access archive for the deposit and dissemination of scientific research documents, whether they are published or not. The documents may come from teaching and research institutions in France or abroad, or from public or private research centers.

L'archive ouverte pluridisciplinaire **HAL**, est destinée au dépôt et à la diffusion de documents scientifiques de niveau recherche, publiés ou non, émanant des établissements d'enseignement et de recherche français ou étrangers, des laboratoires publics ou privés.

**INFLUENCE OF PRESSURE (100 Pa – 100 MPa) ON THE PYROLYSIS
OF AN ALKANE AT MODERATE TEMPERATURE (603 K- 723 K):
EXPERIMENTS AND KINETIC MODELING**

R. Bounaceur ^a, F. Lannuzel ^{a,b}, R. Michels ^b, G. Scacchi ^a, P.-M. Marquaire ^a, V.
Burklé-Vitzthum ^{a,*}

^a Laboratory of Reactions and Process Engineering, LRGP UMR 7274, CNRS,
Université de Lorraine BP 20451, 54001 Nancy, France

^b GeoRessources UMR 7359, CNRS, Université de Lorraine BP 70239, 54501
Vandœuvre-lès-Nancy, France

Corresponding author: valerie.vitzthum@univ-lorraine.fr

Abstract

Confined pyrolysis of *n*-octane was performed in a closed, constant-pressure gold reactor at pressure ranging 1 MPa-70 MPa, temperature between 603 K and 723 K and residence times from 1 hour to 1 month. The main products of reaction are *n*-alkanes of molecular weight lower than *n*-octane and branched alkanes of molecular weight higher than *n*-octane. Alkenes are minor products. At moderate temperature (603 K – 623 K) the conversion of *n*-octane increases with pressure up to a maximum and then decreases (at constant duration of pyrolysis). For higher temperature (723 K) the conversion increases continuously with increasing pressure. A mechanism consisting of 182 free-radical reactions is set up and used to model these experimental results (1-70 MPa) as well as those obtained in a previous study at very low concentration (100 Pa diluted in inert gas, total pressure 0.15 MPa). The agreement between the experimental data and simulation results is satisfactory in terms of product distribution and conversion of *n*-octane in a wide range of pressure (100 Pa to 70 MPa). Some mechanistic explanations concerning the effect of pressure are proposed.

1. Introduction

The pyrolysis of alkanes has been the focus of many studies for a very long time (e.g. [1-7]). The pyrolysis reactions also known as thermal cracking or thermal decomposition are involved in many sectors of chemistry: coal liquefaction (e.g. [8-10]), oil refining (e.g. [11-13]), oil evolution in petroleum reservoirs (e.g. [14-23]), jet-fuels stability for high Mach Number aircrafts [24-27], or deposition of pyrolytic carbon to produce Carbon/Carbon composites by a chemical vapor infiltration process [28-33]. These pyrolysis reactions are of great industrial and commercial importance. The pyrolysis of *n*-alkanes, especially at high pressures (several hundred MPa) has also been of interest to the petroleum geochemistry community. Indeed, laboratory experimentation of the thermal stability of petroleum combined with kinetic modelling is a major methodology aiming to understand the fate of petroleum in geological reservoirs (e.g. [34-42]).

The studies carried out so far focused on very narrow experimental conditions of temperature and/or pressure. The experiments performed at low pressure (about 100 Pa) showed that alkanes and olefins are generated in almost equal quantity [1, 43, 44]. On the other side very few olefins and notable amounts of alkanes are produced in experiments carried out at very high pressure [2, 39, 43, 45-49]. Some authors also studied the influence of pressure on the *n*-alkane conversion. Fabuss et al. [43] gathered numerous results obtained in the range 0.1-100 MPa. They highlighted that pressure up to about 40 MPa increases the pyrolysis rate and pressure above 40 MPa inhibits pyrolysis. Similar conclusions were drawn by Behar and Vandenbroucke [39], and Yu and Eser [50]. Dominé [35] and Dominé et al. [37] focused on the effect of pressure on the products distribution by experimental and modelling studies. Mallinson et al. [51] also conducted a detailed kinetics study of the role of pressure in alkane pyrolysis.

In this study, we intend to establish the link between these various studies by trying to understand how changes in experimental conditions (pressure and temperature) influence the various processes and thus modify the selectivity to products and the conversion of *n*-octane.

We chose octane as the reference alkane to carry out the study of the influence of experimental conditions on the alkane pyrolysis. **Indeed its molecular size allows a rather wide range of smaller and larger products which are easy to analyze by Gas Chromatography.**

This paper presents the experimental procedure and the pyrolysis results of octane at high pressure (1-70 MPa). From these results combined with those of a previous work [52] performed at low concentration (molar fraction 0.07%, partial pressure 100 Pa diluted in Argon – total pressure 0.15MPa), a model of octane pyrolysis based on free radical reactions has been developed to account for experiments from low to high pressure.

2. EXPERIMENTAL SET UP AT HIGH PRESSURE (1-70 MPa)

2.1. Sample

n-octane (purity 99%) was obtained from Aldrich and used as received.

2.2. Confined pyrolysis procedure

Pyrolysis was carried out in gold cells (40 mm length, 5 mm i.d. and 0.5 mm thick). Gold tubes were sealed at one end then filled with 30 mg of sample under helium atmosphere (purity 99.9999%) to avoid the presence of oxygen, and then arc welded at the other end under a refrigerated nitrogen flow in order not to damage the hydrocarbons. The gold cells were loaded in stainless steel autoclaves pressurized at 1, 10 and 70 MPa, while temperature was set in the range 603-723 K, during 1 hour to 1 month (Table 1). At the end

of the pyrolysis, the autoclaves were rapidly (5 min) cooled to room temperature in a water heat exchanger so that cooling time was negligible relative to heating time. For each experimental condition, two or three samples were used for quantitation in order to check the reproducibility and one sample was used for products identification. Details of the confined pyrolysis procedure can be found in [53-56].

2.3. *Identification of products*

Gold cells were pierced, cut in pieces, placed into a vial containing hexane and extracted in an ultrasonic bath for 1 hour. Compounds were identified by gas chromatography–mass spectrometry (HP 5890 Series II GC coupled to a HP 5971 mass spectrometer) using a 60 m DB-5 J&W Scientific, 0.25 mm i.d., 0.1 mm film, fused silica column. The temperature program was 333–433 K at 15 K/min followed by heating to 573 K at 3 K/min.

2.4. *Quantitation of products*

Gold cells were pierced in a vacuum line maintained at 523 K [57]. An aliquot fraction of 0.5 mL was sampled on-line and injected through a heated transfer line into a HP 5890 Series II GC with a 60 m DB-5 J&W Scientific, 0.32 mm i.d, 0.45 μ m film and a fused silica column connected to a flame ionization detector. The temperature program was 273 K during 1 min followed by an increase of 6 K/min up to 573 K. The compounds were quantitated after calibration of the FID using commercially available standards.

3. EXPERIMENTAL RESULTS AT HIGH PRESSURE (1-70 MPa)

3.1. *Reaction products*

An example of chromatogram of the reaction products is presented in Figure 1.

The main reaction products are light *n*-alkanes (of molecular weight lower than that of *n*-octane): CH₄, C₂H₆, C₃H₈, C₄H₁₀, C₅H₁₂ and C₆H₁₄. At the bottom of these peaks, small peaks

which are very difficult to precisely identify are observed. There are mainly alkenes and cycloalkanes.

The molar fractions of the products and *n*-octane obtained after pyrolysis in the different experimental conditions are presented in Supplementary material 1.

The heavy products (mainly C₁₀-C₁₅), in smaller quantity, are composed of branched alkanes. Regarding these compounds, identical series from 3 to 5 peaks can be seen, suggesting a similar mechanism of formation.

3.2. *Influence of pressure and temperature on conversion*

Figure 2 shows the evolution of the conversion obtained under the various experimental conditions. Each data point is the mean value of two or three measurements from two or three experimental replicates; the dispersion of the values can be seen in Supplementary material 1.

It is interesting to note that at 603 K and 623 K, the conversion decreases when the pressure increases at the same reaction time, whereas at 723 K, the opposite phenomenon is observed.

3.3. *Influence of pressure on product distribution*

The reaction products are divided into three families: alkane-minus (alkanes whose molecular weight is lower than that of *n*-octane), alkane-plus (alkanes whose molecular weight is greater than that of *n*-octane) and alkene (alkenes and cycloalkanes). This classification is adopted, because in each family, the compounds are produced by similar free-radical reactions (detailed below).

At high pressure, under our experimental conditions (603 – 723 K), the temperature has a moderate influence on the distribution of the products at identical pressure. The reaction products and their proportion are more or less identical (Table 2).

However the effect of pressure on the products distribution is much more important, in particular on the overall ratio [alkane-minus]/[alkane-plus]. At 603-723 K (Supplementary material 1), the [alkane-minus]/[alkane-plus] ratio is approximatively between 3 and 10 at very high pressure (70 MPa) and increases up to around 100 at lower pressure (1 MPa and 723 K).

4. PYROLYSIS MECHANISM OF A N-ALKANE

Rice, Herzfeld and Kossiakoff [58-60] were the first to explain the thermal cracking of hydrocarbons by a chain reaction mechanism propagated by free radicals at low temperature. Their theory was then confirmed by different teams in low pressure conditions [1, 43, 44] and some others in high pressure conditions [2, 35, 37, 38, 41, 43, 45, 46]. The pyrolysis mechanism constructed in this study was lumped by applying the procedure already described [61, 62].

4.1. *Description of the free-radical reactions*

The different free-radical reactions considered, which compose the lumped pyrolysis mechanism of an *n*-alkane (here *n*-octane), are presented below and in Figure 3:

Unimolecular initiations

The first step, called unimolecular initiation, consists of the formation of two radicals by homolytic bond dissociation. The average Bond Dissociation Energy of the C-C bonds is 82.9 kcal.mol⁻¹ and 96.1 kcal.mol⁻¹ for the C-H bonds [64]. The probability of dissociation of a C-C bond is then 1.300.000 times higher than that of a C-H bond at 573 K and it increases as the temperature decreases. Under our experimental conditions (between 603 K and 723 K), the rate constant of the initiation by C-H bond dissociation is negligible in comparison to the initiation by C-C bond dissociation.

Consequently, it is considered that the initiation step of *n*-octane pyrolysis occurs only by dissociation of the C-C bonds. In the lumped mechanism, it corresponds only to one lumped unimolecular initiation. Indeed, the chain length defined by the ratio of the propagation rates to the initiation rates is always greater than 1000 at moderate temperature (473-773K) ([41, 42, 61] and this study). So the initiation step does not influence the distribution of the products, but the conversion of the reactant (Figure 3), and the initiation reactions can be lumped together.

Decompositions by β -scission

Decompositions by β -scission correspond to unimolecular decompositions of alkyl radicals, which yield a shorter radical and an alkene. Only the decompositions of C-C bonds are taken into account and not the decompositions of C-H bonds, for the same reason than above (Figure 3). All radicals were lumped together according to their number of C atoms.

H-transfers

Only H-transfers between the radicals and the reactant are taken into account. They yield the lumped octyl radical and alkanes (Figure 3).

Additions

The additions of alkyl radicals to alkenes lead to lumped alkyl radicals (Figure 3).

Terminations by recombination

The terminations by recombination of two radicals yield a lumped alkane (Figure 3).

4.2. Construction of the model

The lumped mechanism of *n*-octane pyrolysis includes 182 free radical reactions, implying 33 molecules and 16 radicals. It is presented in the Supplementary Material 2. Intrinsic lumped kinetic parameters are associated with each reaction (frequency factor, A; temperature

coefficient n and activation energy, E_a in mole, cm^3 , s, kcal). The mechanism includes a primary mechanism and a partial secondary mechanism described below.

Primary mechanism

In the primary mechanism, the only molecule that reacts is n -octane (noted $n\text{C}_8$ in the mechanism). The primary mechanism includes 60 reactions: 1 initiation; 16 decompositions by \uparrow -scission of the radicals from C_3 to C_8 (reactions 2 to 17); 7 H-transfers: all the radicals react by H-transfer with n -octane (reactions 18 to 24).

All the termination reactions between all the radicals are written, which represent 36 free-radical reactions.

Secondary mechanism

The primary mechanism enables the modelling of the pyrolysis only at very low conversion (< 5%). For higher conversions, radicals react not only with the initial reactant but also with the reaction products (alkenes and alkanes). Writing an exhaustive secondary mechanism is unmanageable, but a partial secondary mechanism judiciously built makes possible to account for the reaction up to a moderate conversion (about 20%).

The partial secondary mechanism (reactions 61 to 182) is composed of: 1) the additions (39) of all alkyl radicals (from C_2 to C_8) to all alkenes produced in the primary mechanism (from C_2 to C_7); 2) the decompositions by \uparrow -scission (75) of the radicals newly formed by additions; 3) their H-transfers (8) with n -octane.

Estimation of thermochemical and kinetic data

The lumped kinetic parameters are deduced from the intrinsic kinetic parameters calculated by the software EXGAS [63, 64] and the lumping procedure was described elsewhere [61, 62]. **The kinetic parameters were not fitted.**

5. VALIDATION OF THE MODEL

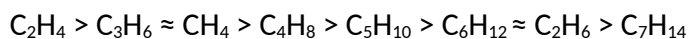
Simulations are performed under the different experimental conditions detailed above using the package of software CHEMKIN II [65], more precisely the SENKIN software at constant pressure and temperature. The lumped kinetic model is tested by comparing the model output with both experimental data obtained in this work at high pressure and at low concentration [52]. The model shows very good agreement with experimental conversion under all conditions. Indeed, the octane conversion is very well described by the model at high pressure (10 and 70 MPa), between 603 and 723K, up to about 20% conversion and more at high temperature (723K). The results of the previous study (100 Pa diluted in inert gas, total pressure 0.15 MPa [52]) are also well simulated by the model at 673 and 723 K, up to about 10% conversion (Figure 2). The experimental molar fractions of the main products ($\text{CH}_4 + \text{C}_2\text{H}_6$, C_3H_8 , $n\text{-C}_4\text{H}_{10}$, $n\text{-C}_5\text{H}_{12}$ and alkanes-plus) were compared to the simulation as a function of octane conversion (up to about 20%) at 603 and 623 K and 10 MPa and 70 MPa (Figure 4). The agreement between the kinetic model and the experimental results is satisfying except for $\text{CH}_4 + \text{C}_2\text{H}_6$ which appear overestimated at 623 K, and the alkanes-plus whose behavior appears more complicated: overestimated at 623 K and 70 MPa, underestimated at 623 K and 10 MPa, and well represented at 603 K. The observed differences could be related to the complexity of analyzing these products: $\text{CH}_4 + \text{C}_2\text{H}_6$ are co-eluted and alkanes-plus correspond to several compounds, each of them being present in small quantity (Figure 1 and Supplementary Material 1). We also tested the mechanism against the experimental conversion of n-octane (Figure 5) and the molar fractions of all products (Figure 6) obtained at low concentration: the agreement between the experimental and the simulation results is satisfying, except for CH_4 which is overestimated by the model. In comparison to the mechanism dedicated to the low concentration previously published

[52], the performance of the new lumped kinetic model is about the same: some species are better represented by the new mechanism (alkenes from C₄ to C₇, ethane), but C₂H₄ and C₃H₆ are now slightly underestimated.

6. DISCUSSION

6.1. *Low pressure versus High pressure conditions and reaction mechanisms.*

A previous experimental study [52] of the pyrolysis of n-octane has been performed at very low reactant concentration (100 Pa diluted in inert gas - total pressure 0.15 MPa) in a closed reactor, at temperatures ranging between 623K and 723K, and reaction time from 1 hour to 70 hours. The major products of the reaction are 1-alkenes (C₂H₄ to C₇H₁₄), methane and ethane; other alkanes (C₃H₈ to C₆H₁₄) are minor products. At 723K and 4 hours, the conversion is close to 10% and we observe, in terms of molar fractions:



These experimental results are very different from those of the thermal decomposition of n-alkanes at the same low temperature but at high pressure. In particular, the cracking stoichiometric equations (for example: C₈H₁₈ = C₆H₁₄ + C₂H₄) are not observed since alkanes (except methane and ethane) are in very low quantities. This can be explained by the very low concentration of reactant which limits the bimolecular reactions. In these conditions, the radicals decompose several times by beta-scissions of C-C bonds when it is possible (unimolecular reaction), rather than react by H-transfers (metathesis) with the reactant (bimolecular reaction) which produce alkanes.

On the contrary, at high pressure, the bimolecular reactions are favored and the alkenes are consumed by addition of alkyl radicals to produce alkanes-plus. So alkenes are only found in trace amounts at high pressure (10 MPa and more).

6.2. Influence of pressure on conversion

At 603 K and 623 K, the conversion decreases when the pressure increases from 10 to 70 MPa for the same reaction time, and so pressure inhibits *n*-octane pyrolysis, whereas at 723 K, the opposite phenomenon is observed, *i.e.* the pyrolysis is accelerated when pressure increases (Figure 2). This behavior was already observed for other *n*-alkanes, from propane to *n*-hexadecane [34, 43, 50, 51]. In order to have a full picture of the pressure effect, the *n*-octane conversion was calculated as a function of pressure at identical reaction time and at 523, 623 and 723 K (Figure 7). At each temperature, the reaction time has been arbitrarily chosen in order to reach a maximum conversion equals to about 50% (1200 years at 523 K, 650 hours at 623 K and 42 minutes at 723 K). The curves at 523 and 623 K are approximately bell-shaped and the maximum increases with increasing pressure. At 723 K the conversion increases continuously with pressure on the whole range of pressure which has been studied.

Some explanations can be suggested. When the pressure increases, the density and the concentration of *n*-octane also increase, and this should lead to the increase of the pyrolysis rate. However, this simple analysis cannot explain the observed phenomenon. Dominé [35] proposed that the effect of pressure results from two phenomena: 1) the rate constants depend on pressure via the activation volume: the rate constants of bimolecular reactions (*i.e.* H-transfers, additions and terminations) increase with pressure, whereas those of unimolecular reactions (*i.e.* initiations and decompositions by \uparrow -scission) decrease when pressure increases. 2) The increase of the *n*-alkane density favors the bimolecular reactions whose rates are the product of two concentrations, relatively to that of unimolecular reactions, whose rates are only proportional to one concentration. A third phenomenon could also play a role in the effect of pressure: the increase in viscosity which hinders the

migration of the species and eventually causes “cage effects”. Nevertheless it is likely that argon which is present in the gold cells considerably lowers the octane viscosity. So the viscosity is probably below the value where the diffusion of the species is limited. The rather high temperatures also limit the increase of viscosity due to high pressure [35, 37]. So the phenomenon of “cage effects” is probably negligible in the experimental conditions. All these phenomena should lead to the decrease of the radical concentration since the initiation reactions are disfavored by pressure and the termination reactions are favored. This would lead to the pyrolysis inhibition.

Moreover the pressure for which the conversion is maximal increases when the temperature increases. Jackson et al. [34] proposed that, at high temperature, the importance of the bimolecular propagation reactions (*i.e.* H-transfers and additions) increases in comparison to the termination reactions whose activation energies are null (Table 3), and this leads to the acceleration of the pyrolysis. Moreover, the increase of temperature makes the initiation reactions easier (Table 3), which leads to the global increase of the concentration of radicals. Both compensate partially for the effect of increasing pressure on the importance of bi vs uni-molecular reactions and shift the maximal conversion to higher pressure.

6.3. *Distribution of the light alkanes at high pressure*

The product distribution obtained by pyrolysis of an *n*-alkane at high pressure (>10 MPa), relatively low temperature (< 723 K) and moderate conversion (< 20%) is similar, whatever the *n*-alkane studied: *n*-octane (this study), *n*-hexadecane [42] or *n*-pentacosane [39]. Particularly, the distribution of *n*-alkanes of molecular weight lower than that of the reactant is approximately bell-shaped (very short alkanes and alkanes close to the reactant in lower amount than the intermediary alkanes).

This section aims to demonstrate that the distribution of the light *n*-alkanes is related to the distribution of the four octyl radicals (called $\mu\cdot$ radicals, Figure 8) in the case of the pyrolysis of *n*-octane.

Figure 9 presents the ratio of the total isomerization rates to the propagation rates, as a function of pressure and temperature. At high pressure and relatively low temperature, which corresponds to the studied conditions, the isomerization reactions are about 50 times faster than the propagation reactions. So the distribution of the $\mu\cdot$ radicals achieves almost its equilibrium value [41], which is directly related to the stability of the radicals: the proportion of a radical increases with its stability. However the stability of an alkyl radical increases with its degree of substitution. It is then possible to classify the 4 octyl radicals according to their stability and therefore their proportion (Figure 10). This assumption is verified by simulation of the kinetic model at 623 K, 70 MPa and 0.1 % conversion. The following proportions, which are in agreement with the previous analysis, are obtained: $\mu_4 = 32.70\%$, $\mu_3 = 32.16\%$, $\mu_2 = 31.63\%$, $\mu_1 = 3.51\%$

It is now possible to explain the distribution of the light *n*-alkanes obtained by pyrolysis of *n*-octane at high pressure. They are produced by the six possible decompositions via \uparrow -scission of the $\mu\cdot$ radicals (Figure 8), which are followed by H-transfers.

Their distribution is related to the relative importance of the various $\mu\cdot$ radicals and the decomposition rate of each of these radicals. The different reactions of $\mu\cdot$ radicals decomposition are represented in Figure 8.

ν The rate r_x of the decomposition reaction x of the radical μ_i is expressed by:

$$r_x = k_x \cdot [\mu_i] \quad (1)$$

If P_i stands for the percentage of the isomer μ_i , and $[\mu\cdot]$ the total concentration of the $\mu\cdot$ radicals, it leads to:

$$[\mu_i] = P_i \cdot [\mu \cdot] \quad (2)$$

And then,

$$r_x = k_x \cdot P_i \cdot [\mu \cdot] \quad (3)$$

The rate constants of the H-transfers which follow the decompositions by \uparrow -scission are very high in comparison to those of the decompositions. So the rate determining steps are the decompositions by \uparrow -scission, the rates of decompositions and H-transfers being equal.

The percentage of the alkane P_x resulting from decomposition x is then equal to:

$$P_x = \frac{r_x}{\sum_x r_x} \quad (4)$$

$$P_x = \frac{k_x \cdot P_i \cdot [\mu \cdot]}{\sum_x k_x \cdot P_i \cdot [\mu \cdot]} \quad (5)$$

$$P_x = \frac{k_x \cdot P_i}{\sum_x k_x \cdot P_i} \quad (6)$$

Thus, we demonstrate that the proportion of the short *n*-alkanes is exclusively linked to the proportion of each μ_i radical and the rate constants of the decompositions.

According to equation (6) and the proportion of the μ_i radicals simulated above, it is thus possible to predict the following distribution of the main products at 623 K, 70 MPa and 72 hours:

$\text{CH}_4 + \text{C}_2\text{H}_6 = 34.7\%$ ($\text{CH}_4 = 2.5\%$, $\text{C}_2\text{H}_6 = 32.2\%$), $\text{C}_3\text{H}_8 = 32.2\%$, $\text{C}_4\text{H}_{10} = 15.8\%$, $\text{C}_5\text{H}_{12} = 15.6\%$,
 $\text{C}_6\text{H}_{14} = 1.7\%$

The calculated selectivity to the short *n*-alkanes (Table 4) is of the same order of magnitude than the experimental selectivity (Table 2), which shows that our former reasoning is globally valid. The selectivity to $\text{CH}_4 + \text{C}_2\text{H}_6$ appears slightly overestimated which could show

that the addition of the corresponding radicals to alkenes could be faster than predicted by the model.

Moreover the experimental selectivity (Table 2) does not depend much on temperature in the studied range. Indeed, the activation energies of the bimolecular isomerizations of the $\mu\cdot$ radicals that determine the $\mu\cdot$ distribution are rather low and so the rate constants are not much sensitive to the temperature.

6.4 Global kinetic parameters

Apparent kinetic parameters (pseudo frequency factor A and pseudo activation energy E_a) were determined by simulation at $T_0 = 523, 603$ and 723 K, under 0.1 MPa, 1 MPa, 10 MPa, 40 MPa and 70 MPa, assuming that cracking reactions follow a first-order kinetic law [e.g. 39]. The initial consumption rates r_0 were calculated by CHEMKIN [for constant conversion \(0.1%\)](#), and by plotting $\ln r_0$ vs $-1/RT$ (where R is the perfect gas constant and T the temperature in K), the slope corresponds to the apparent activation energy. The results are in Table 5 and the activation energies were plotted as a function of the pressure (Figure 11). At 603 and 723 K, when the pressure increases from 0.1 MPa to 70 MPa, the activation energy increases from about 56 kcal/mol to 63 kcal/mol at 603 K and from 51 kcal/mol to 62 kcal/mol at 723 K, and the frequency factor also does. [This is consistent with results of the literature which concern n-butane cracking \[34\]. The kinetic parameters were calculated over a wide range of temperature \(473-873 K\). It was found the activation energy increases from 48.1 kcal/mol at 0.1 MPa to 60.5 kcal/mol at 100 MPa and the frequency factor follows the same trend.](#) The rate constant also increases when the pressure increases but it remains constant from 1 MPa at 603 K and from 10 MPa at 723 K. Rate constants determined at atmospheric pressure can clearly not be used at high pressure. At 523 K, the behavior of the kinetic parameters as a function of pressure is more complicated: the activation energy and

the frequency factor strongly increase up to 10 MPa and then decrease. The rate constant always decreases as a function of pressure. These results are totally consistent with the study of Jackson et al. [34] who also found that the pressure increases rate at high temperatures but it decreases rate at low temperature. So global kinetic parameters strongly depend on pressure and temperature. That is why global kinetic parameters should be handled carefully, especially when they are used for extrapolation, for examples for olefin production at 1000 K or oil cracking at 450 K, which are out of the studied conditions of this paper. The global kinetic parameters must be calculated by simulation of the detailed kinetic model in the conditions range they will be used, if they are not too far from the validation conditions of the model.

Conclusion

Pyrolysis experiments of *n*-octane have been performed at moderate temperature (603-723 K) and high pressure (1 MPa - 70 MPa). The main reaction products are alkanes whose molecular weights are lower than that of *n*-octane, and, in a lower proportion, branched alkanes with higher molecular weight.

A previous experimental study was performed at very low reactant concentration (100 Pa diluted in inert gas - total pressure 0.15 MPa) at temperatures ranging between 623K and 723K. The major products are 1-alkenes (C_2H_4 to C_7H_{14}), methane and ethane; other alkanes (C_3H_8 to C_6H_{14}) are minor products.

On the basis of both studies, a kinetic mechanism of *n*-octane pyrolysis has been developed which describes the reaction products and the conversion on a very large range of pressure. This model has been validated by comparison with the experimental results presented herein and a previous experimental study performed at much lower pressure.

The distribution of the main products at high pressure has also been investigated. It is related

to the isomerization reactions of the octyl radicals. These reactions determine the distribution of the octyl radicals, which directly determines the products distribution.

The pressure has a particular effect on the *n*-octane conversion: at moderate temperature the conversion increases with pressure up to a maximum and then decreases, and, at higher temperature, the conversion seems increasing continuously with pressure. Some explanations have been proposed in this paper, but a detailed kinetic analysis will be helpful to precisely highlight the reasons of the complex effect of pressure.

Acknowledgment

This work was supported by TOTAL—Exploration & Production (Pau, France).

REFERENCES

- [1] H.H. Voge, G.M. Good, Thermal cracking of higher paraffins, *J. Am. Chem. Soc.* 71 (1949) 593–597.
- [2] B.M. Fabuss, J.O. Smith, R.I. Lait, A.S. Borsanyi, C.N. Satterfield, Rapid thermal cracking of n-hexadecane at elevated pressures, *Ind. Eng. Chem. Process Des. Dev.* 1 (1962) 293-299.
- [3] E. Ranzi, M. Dente, S. Pierucci, G. Biardi, Initial product distributions from pyrolysis of normal and branched paraffins, *Ind. Eng. Chem. Fundam.* 22 (1983) 132–139.
- [4] F. Baronnet, M. Niclause, Industrial problems and basic research in pyrolysis and oxidation reactions, *Ind. Eng. Chem. Fundam.* 25 (1986) 9-19.
- [5] F. Khorasheh, M.R. Gray, 1993. High-pressure thermal cracking of n-hexadecane. *Ind. Eng. Chem. Res.* 32, 1853–1863.
- [6] M.L. Poutsma, Fundamental reactions of free radicals relevant to pyrolysis reactions, *J. Anal. Appl. Pyrolysis* 54 (2000) 5–35.
- [7] P.E. Savage, Mechanisms and kinetics models for hydrocarbon pyrolysis, *J. Anal. Appl. Pyrolysis* 54 (2000) 109–126.
- [8] M.T. Martinez, A.M. Benito, M.A. Callejas, Thermal cracking of coal residues: Kinetics of asphaltene decomposition, *Fuel* 76 (1997) 871-877.
- [9] M.T. Martinez, A.M. Benito, M.A. Callejas, Kinetics of asphaltene hydroconversion .1. Thermal hydrocracking of a coal residue, *Fuel* 76 (1997) 899-905.
- [10] B.E. Hartman, P.G. Hatcher, Valuable Crude Oil from Hydrothermal Liquefaction of an Aliphatic Coal, *Energy Fuels* 28 (2014) 7538-7551.
- [11] M. Dente, S. Pierucci, E. Ranzi, G. Bussani, New improvements in modeling kinetic schemes for hydrocarbons pyrolysis reactors, *Chem. Eng. Sci.* 47 (1992) 2629-2634.

- [12] E. Ranzi, M. Dente, M. Rovaglio, T. Faravelli, S.B. Karra, Pyrolysis and chlorination of small hydrocarbons, *Chem. Eng. Commun.* 117 (1992) 17-39.
- [13] S. Wauters, G.B., Marin, Kinetic modeling of coke formation during steam cracking, *Ind. Eng. Chem. Res.* 41 (2002) 2379-2391.
- [14] P. Ungerer, R. Pelet, Extrapolation of the kinetics of oil and gas formation from laboratory experiments to sedimentary basins, *Nature* 327 (1987) 52-54.
- [15] P. Ungerer, F. Béhar, M. Villalba, O.R. Heum, A., Audibert, Kinetic modelling of oil cracking, *Org. Geochem.* 13 (1988) 857-868.
- [16] F. Béhar, S. Kressmann, J.L. Rudkiewicz, M. Vandenbroucke, Experimental simulation in a confined system and kinetic modelling of kerogen and oil cracking, *Org. Geochem.* 19 (1992) 173-189.
- [17] H.J. Schenk, R. Di Primio, B. Horsfield, The conversion of oil into gas in petroleum reservoirs. Part I: Comparative kinetic investigation of gas generation from crude oils of lacustrine, marine and fluviodeltaic origin by programmed-temperature closed system pyrolysis, *Org. Geochem.* 26 (1997) 467-481.
- [18] M. Vandenbroucke, F. Béhar, J.L. Rudkiewicz, Kinetic modelling of petroleum formation and cracking: implications from the high pressure/high temperature Elgin Field (UK, North Sea), *Org. Geochem.* 30 (1999) 1105-1125.
- [19] F. Béhar, H. Budzinski, M. Vandenbroucke, Y. Tang, Methane generation from oil cracking: Kinetics of 9-methylphenanthrene cracking and comparison with other pure compounds and oil fractions, *Energy Fuels* 13 (1999) 471-481.
- [20] D.W. Waples, The kinetics of in-reservoir oil destruction and gas formation: constraints from experimental and empirical data, and from thermodynamics, *Org. Geochem.* 31 (2000) 553-575.

- [21] T. Al Darouich, F. Béhar, C. Largeau, Thermal cracking of the light aromatic fraction of Safaniya crude oil - experimental study and compositional modelling of molecular classes, *Org. Geochem.* 37 (2006) 1130-1154.
- [22] T. Al Darouich, F. Béhar, C. Largeau, Pressure effect on the thermal cracking of the light aromatic fraction of Safaniya crude oil - implications for deep prospects, *Org. Geochem.* 37 (2006) 1155-1169.
- [23] F. Béhar, F. Lorant, L. Mazeas, Elaboration of a new compositional kinetic schema for oil cracking, *Org. Geochem.* 39 (2008) 764-782.
- [24] T.A. Ward, J.S. Ervin, S. Zabarnick, L. Shafer, Pressure effects on flowing mildly-cracked n-decane, *J. Propul. Power* 21 (2005) 344-355.
- [25] T. Edwards, Cracking and deposition behavior of supercritical hydrocarbon aviation fuels, *Combust. Sci. Technol.* 178 (2006) 307-334.
- [26] S. Humer, A. Frassoldati, S. Granata, T. Faravelli, E. Ranzi, R. Seiser, K. Seshadri, Experimental and kinetic modeling study of combustion of JP-8, its surrogates and reference components in laminar nonpremixed flows, *Proc. Combust. Inst.* 31 (2007) 393-400.
- [27] O. Herbinet, P.M. Marquaire, F. Battin-Leclerc, R. Fournet, Thermal decomposition of n-dodecane: Experiments and kinetic modeling, *J. Anal. Appl. Pyrolysis* 78 (2007) 419-429.
- [28] K. Norinaga, O. Deutschmann, Detailed kinetic modeling of gas-phase reactions in the chemical vapor deposition of carbon from light hydrocarbons, *Ind. Eng. Chem. Res.* 46 (2007) 3547-3557.
- [29] I. Ziegler, R. Fournet, P.M. Marquaire, Pyrolysis of propane for CVI of pyrocarbon: Part I. Experimental and modeling study of the formation of toluene and aliphatic

- species, *J. Anal. Appl. Pyrolysis* 73 (2005) 212–230.
- [30] I. Ziegler, R. Fournet, P.M. Marquaire, Pyrolysis of propane for CVI of pyrocarbon: Part II. Experimental and modeling study of polyaromatic species, *J. Anal. Appl. Pyrolysis* 73 (2005) 231–247.
- [31] I. Ziegler-Devin, R. Fournet, P.M. Marquaire, Pyrolysis of propane for CVI of pyrocarbon: Part III. Experimental and modeling study of the formation of pyrocarbon, *J. Anal. Appl. Pyrolysis* 79 (2006) 268-277.
- [32] I. Ziegler-Devin, R. Fournet, R. Lacroix, P.M. Marquaire, Pyrolysis of propane for CVI of pyrocarbon: Part IV. Main Pathways involved in pyrocarbon deposit, *J. Anal. Appl. Pyrolysis* 104 (2013) 48-58.
- [33] R. Lacroix, R. Fournet, I. Ziegler-Devin, P.M. Marquaire, Kinetic modeling of surface reactions involved in CVI of pyrocarbon obtained by propane pyrolysis, *Carbon* 48 (2010) 132-144.
- [34] K.J. Jackson, A.K. Burnham, R.L. Braun, K.G. Knauss, Temperature and pressure dependence of n-hexadecane cracking, *Org. Geochem.* 23 (1995) 941–953.
- [35] F. Domine, Kinetics of hexane pyrolysis at very high pressures, 1. Experimental study. *Energy Fuels* 3 (1989) 89-96.
- [36] F. Domine, High-pressure pyrolysis of n-hexane, 2,4-dimethylpentane and 1-phenylbutane - Is pressure an important geochemical parameter? *Org. Geochem.* 17 (1991) 619-634.
- [37] F. Domine, P.M. Marquaire, C. Muller, G.M. Come, Kinetics of hexane pyrolysis at very high pressures, 2. Computer modeling. *Energy Fuels* 4 (1990) 2-10.
- [38] F. Domine, F. Enguehard, Kinetics of hexane pyrolysis at very high pressures–3. Application to geochemical modeling, *Org. Geochem.* 18 (1992) 41-49.

- [39] F. Béhar, M. Vandenbroucke, M., Experimental determination of the rate constants of the n-C25 thermal cracking at 120, 400 and 800 bar: implications for the high pressure/high temperature prospects, *Energy Fuels* 10 (1996) 932-940.
- [40] A.K. Burnham, H.R. Gregg, R.L. Ward, K.G. Knauss, S.A. Copenhaver, J.G. Reynolds, R. Sanborn, Decomposition kinetics and mechanism of n-hexadecane-1,2-13C2 and dodec-1-ene-1,2-13C2 doped in petroleum and n-hexadecane, *Geochim. Cosmochim. Acta* 61 (1997) 3725-3737.
- [41] R. Bounaceur, V. Warth, P.M. Marquaire, G. Scacchi, F. Dominé, D. Dessort, B. Pradier, O. Brevart, Modeling of hydrocarbons pyrolysis at low temperature. Automatic generation of free radicals mechanisms, *J. Anal. Appl. Pyrolysis* 64 (2002) 103-122.
- [42] V. Burklé-Vitzthum, R. Michels, G. Scacchi, P.M. Marquaire, D., Dessort, B. Pradier, O. Brévar, Kinetic Effect of Alkylaromatics on the Thermal Stability of Hydrocarbons under Geological Temperatures, *Org. Geochem.* 35 (2004) 3-31.
- [43] B.M. Fabuss, J.O. Smith, C.N. Satterfield, Thermal cracking of pure saturated hydrocarbons, *Adv. Petrol. Chem. Refining* 3 (1964) 156-201.
- [44] D. Depeyre, C. Flicoteaux, C. Chardaire, Pure n-hexadecane thermal steam cracking, *Ind. Eng. Chem. Process Des. Dev.* 24 (1985) 1251-1258.
- [45] F. Doue, G. Guiochon, Etude theorique et experimentale de la cinetique de decomposition thermique du n-hexadecane, de son mecanisme et de la composition du melange des produits obtenus, *Journal de Chimie-Physique* 65 (1968) 395.
- [46] F. Doue, G. Guiochon, The Formation of Alkanes in the Pyrolysis of n-hexadecane: Effect of an Inert Gas on the Decomposition of Alkyl Radicals, *Can. J. Chem.* 47 (1969) 3477-3480.

- [47] J. Shabtai, R. Ramakrishnan, A.G. Oblad, Hydropyrolysis of Model Compounds, In Thermal Hydrocarbon Chemistry, Adv. Chem. Ser. 183 (1979) 297–329.
- [48] T.J. Ford, Liquid-phase thermal decomposition of hexadecane: reaction mechanisms, Ind. Eng. Chem. Fundam. 25 (1986) 240–243.
- [49] P. Zhou, B.L. Crynes, Thermolytic reactions of dodecane, Ind. Eng. Chem. Process Des. Dev. 25 (1986) 508–514.
- [50] J. Yu, S. Eser, Kinetics of Supercritical-Phase Thermal Decomposition of C10-C14 Normal Alkanes and Their Mixtures, Ind. Eng. Chem. Res. 36 (1997) 585–591.
- [51] R.G. Mallinson, R.L. Braun, C.K. Westbrook, A.K. Burnham, Detailed chemical kinetics study of the role of pressure in butane pyrolysis, Ind. Eng. Chem. Res. 31 (1992) 37–45.
- [52] N. Razafinarivo, R. Bounaceur, V. Burklé-Vitzthum, F. Lannuzel, R. Michels, G. Scacchi, P.M. Marquaire, Pyrolysis of n-octane at very low concentration and low temperature, J. Anal. Appl. Pyrolysis 117 (2016) 282-289.
- [53] P. Landais, M. Monthioux, Closed system pyrolysis: an efficient technique for simulating natural coal maturation, Fuel Process. Technol. 20 (1988) 123-132.
- [54] P. Landais, R. Michels, B. Poty, M. Monthioux, Pyrolysis of organic matter in cold-seal pressure autoclaves. Experimental approach and applications, J. Anal. Appl. Pyrolysis 16 (1989) 103-115.
- [55] R. Michels, P. Landais, Artificial coalification: Comparison of confined pyrolysis and hydrous pyrolysis, Fuel 73 (1994) 1691–1696.
- [56] R. Michels, P. Landais, R.P. Philp, B.E. Torkelson, Influence of pressure and the presence of water on the evolution of the residual kerogen during confined, hydrous, and high-pressure hydrous pyrolysis of Woodford shale, Energy Fuels 9 (1995) 204–

215.

- [57] L. Gerard, M. Elie, P. Landais, Analysis of confined pyrolysis effluents by thermodesorption multidimensional gas chromatography, *J. Anal. Appl. Pyrolysis* 29 (1994) 137-152.
- [58] F.O. Rice, The thermal decomposition of organic compounds from the standpoint of free radicals. III. The calculation of the products formed from paraffin hydrocarbons, *J. Am. Chem. Soc.* 55 (1933) 3035-3040.
- [59] F.O. Rice, K.F. Herzfeld, The thermal decomposition of organic compounds from the standpoint of free radicals. VI. The mechanism of some chain reactions, *J. Am. Chem. Soc.* 56 (1934) 284-289.
- [60] A. Kossiakoff, F.O. Rice, Thermal Decomposition of Hydrocarbons: Resonance Stabilization and Isomerization of Free Radicals 1, *J. Am. Chem. Soc.* 65 (1943) 590-595.
- [61] V. Burklé-Vitzthum, R. Bounaceur, P.M. Marquaire, F. Montel, L. Fusetti, Thermal evolution of n- and iso-alkanes in oils. Part 1: Pyrolysis model for a mixture of 78 alkanes (C1-C32) including 13,206 free radical reactions, *Org. Geochem.* 42 (2011) 439-450.
- [62] F. Dominé, R. Bounaceur, G. Scacchi, P.M. Marquaire, D. Dessort, B. Pradier, O. Brevart, Up to what temperature is petroleum stable? New insights from a 5200 free radical reactions model, *Org. Geochem.* 33 (2002) 1487-1499.
- [63] V. Warth, N. Stef, P.A. Glaude, F. Battin-Leclerc, G. Scacchi, G.M. Côme, Computer-aided derivation of gas-phase oxidation mechanisms: Application to the modeling of the oxidation of n-butane, *Combust. Flame* 114 (1998) 81-102.
- [64] S.W. Benson, Methods for the estimation of thermochemical data and rate

parameters, John Wiley & Sons, New York, 1976.

- [65] R. J. Kee, F.M. Rupley, J.A. Miller, Chemkin-II: A fortran chemical kinetics package for the analysis of gas phase chemical kinetics, SAND-89-8009, Sandia National Labs., Livermore, CA (USA), 1989.

Figure captions

Figure 1. Chromatogram obtained after pyrolysis of *n*-octane at 623 K, 70 MPa and 5 days. The compounds observed are typical of the octane pyrolysis obtained in this study. Compound identification by names or formulae. Unlabelled peaks are iso-alkanes isomers of the identified peaks. The very small peaks are alkenes and cycloalkanes.

Figure 2. Conversion of *n*-octane as a function of time, obtained after pyrolysis at high pressure: experimental (markers) and simulation results (solid lines). Experimental and modelling data at 100 Pa from Razafinarivo et al. (2016). Note the inversed effects of pressure on conversion when temperature increases.

Figure 3. Examples of free-radical reactions taken into account in the pyrolysis mechanism of *n*-octane.

Figure 4. Experimental (markers) and simulation (solid lines) results: evolution of the molar fractions of the products as a function of *n*-octane conversion at 603K and 623 K, at 10 MPa and 70 MPa.

Figure 5. Experimental (markers) and simulation (solid lines) results: evolution of the *n*-octane conversion as a function of time at 673K and 723 K, and a partial pressure of 100 Pa (total pressure 0.15 MPa).

Figure 6. Experimental (markers) and simulation (solid lines) results: evolution of the molar fractions of the products as a function of time at 723 K, and a partial pressure of 100 Pa (total pressure 0.15 MPa).

Figure 7. Simulated *n*-octane conversion as a function of pressure at identical reaction time (1200 years at 523 K, 650 hours at 623 K and 42 minutes at 723 K).

Figure 8. The six decompositions by β -scission of the μ · radicals with assigned rate constants k .

Figure 9. Ratio of the total isomerization rates to the propagation rates, as a function of temperature and pressure ([simulation results](#)).

Figure 10. Classification of the 4 octyl radicals according to their relative stability.

Figure 11. Calculated global activation energy as a function of pressure and temperature for octane cracking ([simulation results](#)).

Table captions

Table 1. Experimental conditions of high pressure pyrolysis of *n*-octane.

Table 2. Experimental selectivity (mol %) of the short *n*-alkanes as a function of pressure and temperature.

Table 3. Ratio of the rate constants (initiations to terminations, H-transfers to terminations and additions to terminations) at 523, 623 and 723 K ([simulation results](#)).

Table 4. Calculated selectivity (mol %) of the short *n*-alkanes as a function of pressure and temperature ([simulation results](#)).

Table 5. Calculated activation energy and frequency factor at 723 K ([simulation results](#)).

Captions of the supplementary material

Supplementary material 1. Molar fractions of the reactant and the main products obtained after pyrolysis of *n*-octane.

Supplementary material 2. Lumped kinetic model of the pyrolysis of *n*-octane.

Figure 1.

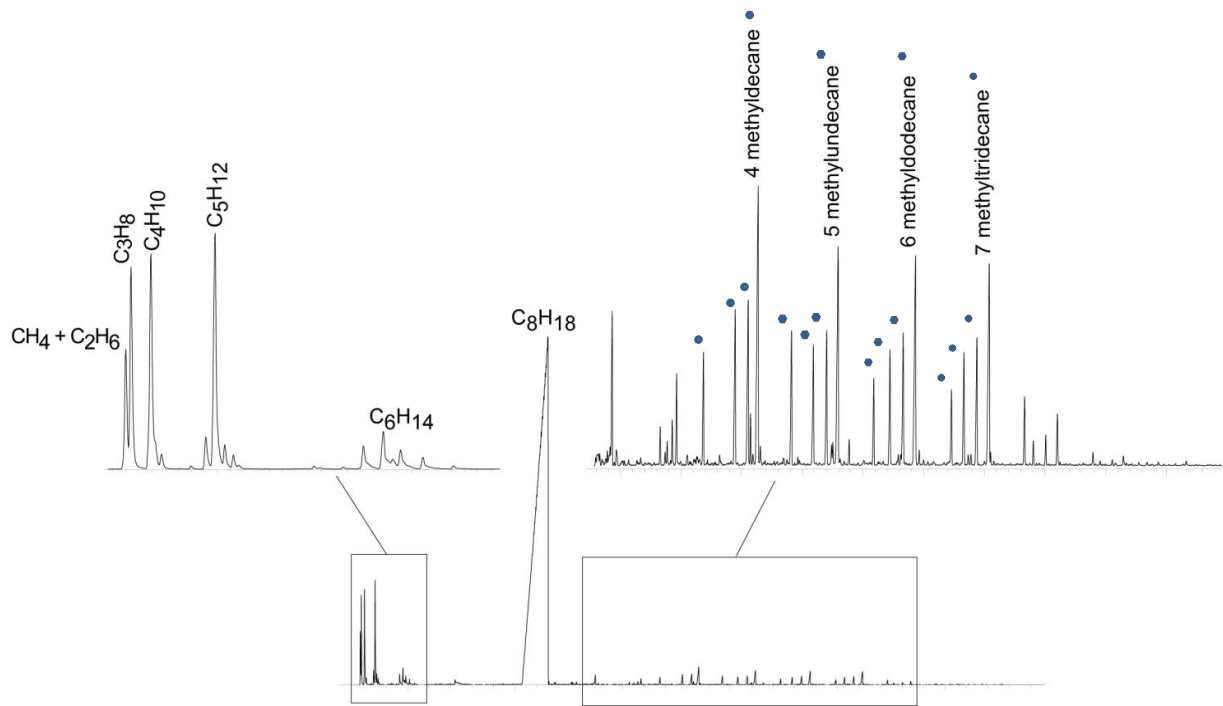
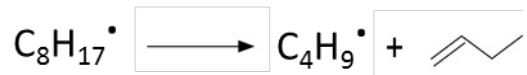


Figure 3.

Lumped unimolecular initiation:



Example of lumped decomposition by β -scission:



Example of lumped H-transfer:



Example of lumped addition:



Example of lumped termination by recombination:

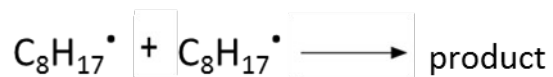


Figure 8.

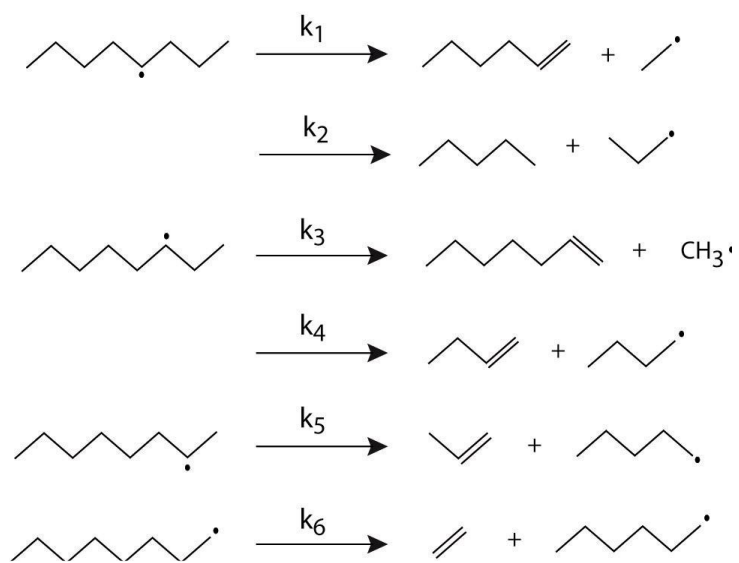


Figure 9. Ratio of the total isomerization rates to the propagation rates, as a function of temperature and pressure (simulation results).

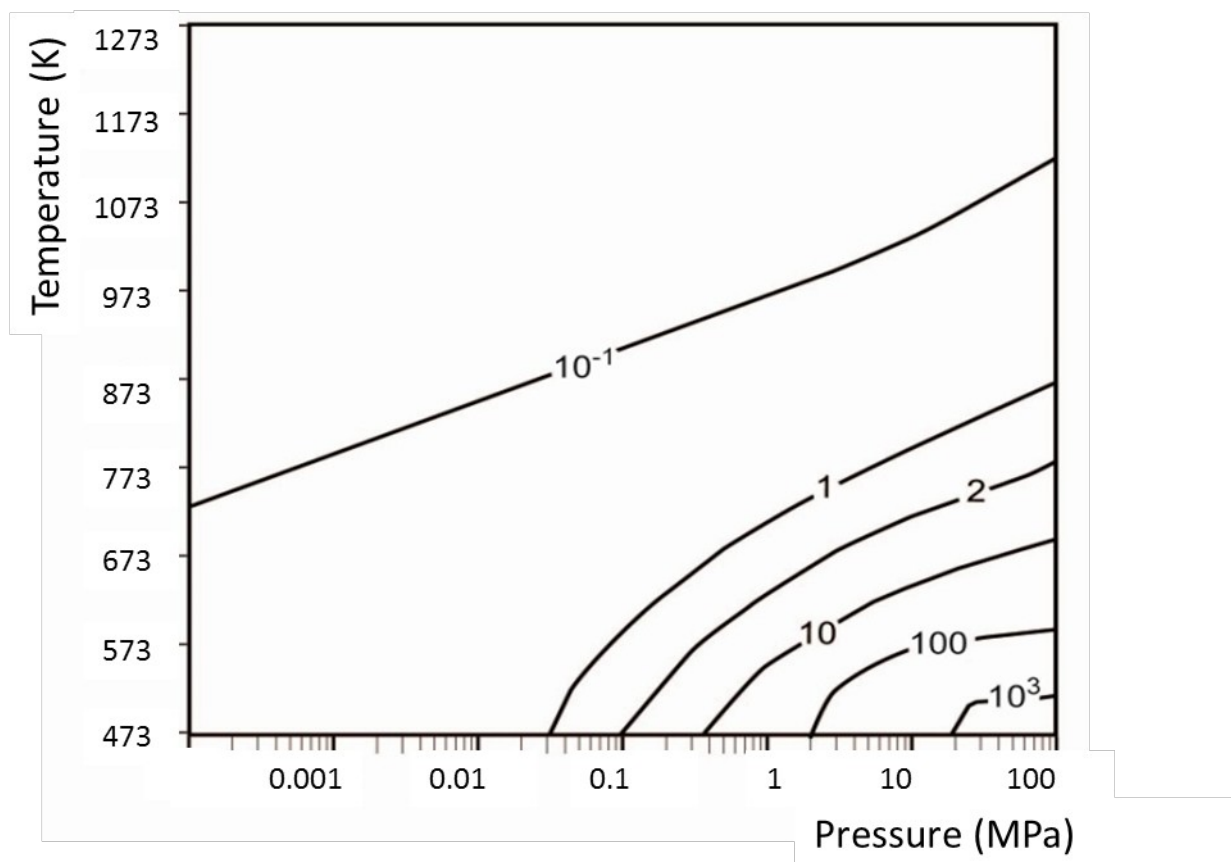


Figure 10.

Table 1. Experimental conditions of high pressure pyrolysis of *n*-octane.

Temperature	Pressure	Time
603 K	70 MPa	From 3 days to 1 month
603 K	10 MPa	From 3 days to 1 month
623 K	70 MPa	From 3 days to 1 week
623 K	10 MPa	From 3 days to 1 week
723 K	70 MPa	From 1 hour to 3 hours
723 K	1 MPa	From 1 hour to 3 hours

Table 2. Experimental selectivity (mol %) of the short *n*-alkanes as a function of pressure and temperature.

Conditions			Selectivity of the short <i>n</i> -alkanes (mol %)				
Temperature	Pressure	Time	CH ₄ + C ₂ H ₆	C ₃ H ₈	C ₄ H ₁₀	C ₅ H ₁₂	C ₆ H ₁₄
723 K	70 MPa	1 hr	25.1	27.9	24.1	17.3	5.6
623 K	70 MPa	72 hrs	18.3±2.9	31.2±2.5	23.9±2.1	26.8±2.0	≈0.0
603 K	70 MPa	72 hrs	25.2	26.3	25.2	18.9	4.4
623 K	10 MPa	72 hrs	14.9	27.2	29.9	21.6	6.4
603 K	10 MPa	72 hrs	16.0	30.9	25.9	21.2	6.0

Table 3. Ratio of the rate constants (initiations to terminations, H-transfers to terminations and additions to terminations) at 523, 623 and 723 K ([simulation results](#)).

Temperature	$k_{\text{initiation/termination}}$ (mol.cm ⁻³)	$k_{\text{H-transfer/termination}}$ (no unit)	$k_{\text{addition/termination}}$ (no unit)
523 K	5.8×10^{-33}	5.8×10^{-07}	3.4×10^{-05}
623 K	3.2×10^{-27}	3.1×10^{-06}	1.2×10^{-04}
723 K	4.5×10^{-23}	1.1×10^{-05}	2.9×10^{-04}

Table 4. Calculated selectivity (mol %) of the short *n*-alkanes as a function of pressure and temperature ([simulation results](#)).

Conditions			Selectivity of the short <i>n</i> -alkanes (mol %)				
Temperature	Pressure	Time	CH ₄ + C ₂ H ₆	C ₃ H ₈	C ₄ H ₁₀	C ₅ H ₁₂	C ₆ H ₁₄
723 K	70 MPa	1 hour	32.3	27.2	16.6	19.1	4.8
623 K	70 MPa	72 hours	34	31.6	16.3	16.2	1.9
603 K	70 MPa	72 hours	34.1	31.8	16.3	16.1	1.7
623 K	10 MPa	72 hours	32.8	29.5	17.0	17.8	2.9
603 K	10 MPa	72 hours	33.2	30.5	16.9	17.1	2.3

Table 5. Calculated global activation energy and frequency factor (simulation results).

Temperature (K)	Pressure (MPa)	Frequency factor (s ⁻¹)	Activation energy (kcal/mol)	Rate constant (s ⁻¹)
523	0.1	1.3×10 ¹⁴	60.5	6.8×10 ⁻¹²
	1	2.2×10 ¹⁴	61.1	6.4×10 ⁻¹²
	10	3.2×10 ¹⁹	74.0	3.8×10 ⁻¹²
	40	6.7×10 ¹⁸	72.9	2.3×10 ⁻¹²
	70	2.9×10 ¹⁸	72.3	1.8×10 ⁻¹²
603	0.1	3.8×10 ¹²	56.4	1.4×10 ⁻⁰⁸
	1	8.0×10 ¹³	59.6	2.0×10 ⁻⁰⁸
	10	3.6×10 ¹⁴	61.4	2.0×10 ⁻⁰⁸
	40	6.7×10 ¹⁴	62.2	1.9×10 ⁻⁰⁸
	70	1.5×10 ¹⁵	63.2	1.9×10 ⁻⁰⁸
723	0.1	8.1×10 ¹⁰	51.1	2.9×10 ⁻⁰⁵
	1	1.6×10 ¹²	54.2	6.6×10 ⁻⁰⁵
	10	4.4×10 ¹³	58.2	11×10 ⁻⁰⁵
	40	3.4×10 ¹⁴	61.0	12×10 ⁻⁰⁵
	70	5.6×10 ¹⁴	61.7	12×10 ⁻⁰⁵

Supplementary material 1. Molar fractions of the reactant and the main products obtained after pyrolysis of *n*-octane.

723 K	70 MPa	Time (hours)	CH ₄ +C ₂ H ₆	C ₃ H ₈	C ₄ H ₁₀	C ₅ H ₁₂	C ₆ H ₁₄	C ₈ H ₁₈	Conversion (%)	Alkanes-plus	[alkane-minus]/[alkane-plus]	C balance
		1	0.135 ±0.005	0.150 ±0.005	0.130 ±0.005	0.0935 ±0.0005	0.030 ±0.005	0.200 ±0.010	80±1	0.195 ±0.015	2.8	75.3%
		3	0.210 ±0.010	0.220 ±0.010	0.155 ±0.005	0.092 ±0.002	0.025 ±0.005	0.060 ±0.010	94±1	0.38 ±0.010	10.3	96.6%

623 K	70 MPa	Time (hours)	CH ₄ +C ₂ H ₆	C ₃ H ₈	C ₄ H ₁₀	C ₅ H ₁₂	C ₆ H ₁₄	C ₈ H ₁₈	Conversion (%)	Alkanes-plus	[alkane-minus]/[alkane-plus]	C balance
		72	0.010 ±0.001	0.0170 ±0.005	0.0130 ±0.005	0.0145 ±0.005	trace	0.935 ±0.005	6.23 ±0.70	0.010 ±0.001	5.5	97.6%
		120	0.0115 ±0.0015	0.019 ±0.002	0.0155 ±0.005	0.019 ±0.001	trace	0.91 ±0.01	9.17 ±0.87	0.0185 ±0.0005	3.5	97.0%
		168	0.027 ±0.005	0.050 ±0.010	0.039 ±0.008	0.042 ±0.006	trace	0.84 ±0.02	15.61 ±2.05	0.0245 ±0.0015	6.4	95.1%

603 K	70 MPa	Time (hours)	CH ₄ +C ₂ H ₆	C ₃ H ₈	C ₄ H ₁₀	C ₅ H ₁₂	C ₆ H ₁₄	C ₈ H ₁₈	Conversion (%)	Alkanes-plus	[alkane-minus]/[alkane-plus]	C balance
		72	0.0012 ±0.0003	0.00125 ±0.00015	0.0012 ±0.0002	0.0009 ±0.0001	0.00021 ±0.00007	0.990 ±0.005	0.81 ±0.08	0.0020 ±0.0003	2.4	99.5%
		120	0.0020 ±0.0003	0.0028 ±0.0003	0.0025 ±0.0001	0.0021 ±0.0001	0.00034 ±0.00017	0.980 ±0.005	1.81 ±0.11	0.0048 ±0.0008	2.0	99.2%

623 K	10 MPa	Time (hours)	CH ₄ +C ₂ H ₆	C ₃ H ₈	C ₄ H ₁₀	C ₅ H ₁₂	C ₆ H ₁₄	C ₈ H ₁₈	Conversion (%)	Alkanes-plus	[alkane-minus]/[alkane-plus]	C balance
		72	0.004 ±0.001	0.0073 ±0.0013	0.008 ±0.002	0.0058 ±0.0014	0.0017 ±0.0002	0.95 ±0.01	5.66 ±0.86	0.008 ±0.003	3.4	97.6%
		120	0.018 ±0.008	0.0236 ±0.007	0.027 ±0.008	0.0180 ±0.0023	0.0039 ±0.0012	0.86 ±0.03	13.36 ±3.38	0.020 ±0.003	4.5	93.4%

603 K	10 MPa	Time (hours)	CH ₄ +C ₂ H ₆	C ₃ H ₈	C ₄ H ₁₀	C ₅ H ₁₂	C ₆ H ₁₄	C ₈ H ₁₈	Conversion (%)	Alkanes-plus	[alkane-minus]/[alkane-plus]	C balance
		72	0.0008 ±0.0001	0.00155 ±0.00025	0.0013 ±0.0003	0.00106 ±0.00019	0.00030 ±0.00008	0.991 ±0.001	0.91 ±0.13	0.00024 ±0.0001	2.1	99.4%
		168	0.00185 ±0.00035	0.00315 ±0.00065	0.0027 ±0.0007	0.00222 ±0.00051	0.000495 ±0.000085	0.982 ±0.005	1.77 ±0.44	0.00078 ±0.0003	1.3	98.8%

